ACS Macro Letters

Letter

Cite This: ACS Macro Lett. 2018, 7, 699−704

pubs.acs.org/macroletters

Local Structure and Relaxation Dynamics in the Brush of Polymer-Grafted Silica Nanoparticles

Yuan Wei,[†] Yifan Xu,[†] Antonio Faraone,[‡] and Michael J. A. Hore*[,†]

[†]Department of Macromolecular Science & Engineering, Case Western Reserve University, 10900 Euclid Avenue, Cleveland, Ohio 44106, United States

[‡]NIST Center for Neutron Research, National Institute of Standards and Technology, Gaithersburg, Maryland 20899, United States

Supporting Information

ABSTRACT: When grafted to spherical nanoparticles at high grafting densities, polymers adopt a variety of conformations. Because of strong confinement by neighboring chains, portions of the polymer near the nanoparticle core are highly stretched in the concentrated polymer brush region (CPB) of the polymer layer. Farther away from the core, where the polymer is less confined, the conformation becomes more ideal in the semidilute polymer brush (SDPB) region. Using a combination of small-angle neutron scattering (SANS) and neutron spin echo (NSE) spectroscopy, we directly characterized both the structure and dynamics of the CPB and SDPB on poly(methyl acrylate) (PMA) grafted SiO_2 nanoparticles (NPs). Analysis of SANS measurements using a new core-chain-chain (CCC) model confirmed that the portion of the chain in the CPB region is highly stretched, and transitions to a more random conformation. Dynamics in the CPB region were found to be much slower than the SDPB region.

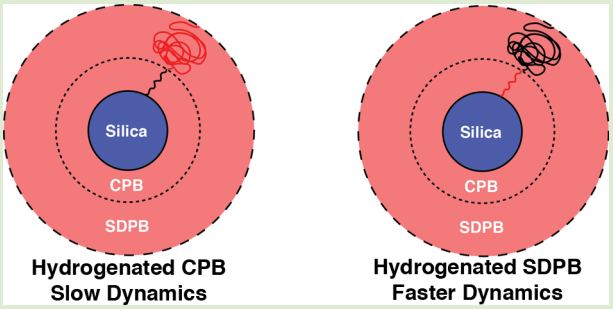

Polymer chains are grafted to NP surfaces for a variety of purposes, including altering the NP solubility, dispersion within a polymer matrix, or to suppress immune responses to the NPs in biological applications.[1−4] Polymers grafted to planar substrates typically form a polymer brush, characterized by a dense layer of stretched polymer chains. In the past few decades, polymer brushes have been the subject of a great deal of research to understand their structure, dynamics, and behavior.

In the case of polymer-grafted nanospheres, the structure of the polymer brush is more complex than the case of planar substrates, and several studies have sought to characterize the structure of the brush on grafted nanospheres.[5−14] At low grafting densities in the "mushroom regime", the grafted chain conformation remains ideal, and the radius of gyration of the chain scales with the degree of polymerization as $R_g \sim N^{\nu}$, where the excluded volume parameter (i.e., Flory exponent) is between $\nu = 0.5$ and $\nu = 0.6$. Dynamic light scattering (DLS) measurements by Ohno et al.[5] of the hydrodynamic radius (R_h) of poly(methyl methacrylate) (PMMA)-grafted, silica (SiO_2) NPs with a core radius $r_{core} = 65$ nm found that at high grafting densities ($\sigma > 0.6$ chains/nm^2), the brush thickness h scaled with the molecular weight as $h \sim M_w^{0.85}$ for low molecular weights, but transitioned to the expected scaling relation $h \sim M_w^{0.6}$ as the molecular weight increased. Dukes et al.[6] found similar scaling relationships from DLS measurements, and Choi et al.[7,8] observed that for the case of no excluded volume, the grafted chains transition to a Gaussian conformation at high molecular weights with $h \sim N^{0.5}$. Recently, Hore et al.[9] directly measured the structure of PMMA-grafted Fe_3O_4 NPs by small-angle neutron scattering (SANS) measurements fit to a core−shell-chain form factor, and found evidence of a dense PMMA layer near the NP core, that transitioned to a less dense layer with a size that scaled as $R_g \sim N^{0.5}$. The presence of two regimes of polymer conformation is due to an increase in the accessible volume for a polymer chain as the distance from the NP surface increases, resulting in a high concentration of strongly confined chains near the NP surface (concentrated polymer brush region, CPB) that become less confined as the distance from the NP surface increases (semidilute polymer brush region, SDPB). The presence of two concentration regimes follows from extension of the Daoud−Cotton model to include the nanoparticle core,[15] giving rise to a cutoff distance r_c between the CPB and SDPB regions:

$$r_c = \frac{r_{core}\sqrt{\sigma^*}}{\nu^*} \tag{1}$$

where $\sigma^* = \sigma b^2$ is the grafting density multiplied by the square of the Kuhn length (b), $\nu^* = \nu/\sqrt{4\pi}$ is a rescaled excluded volume parameter, and r_{core} is the NP radius.[5,6] If $r_c < r_{core}$, then no CPB region exists. SCFT calculations by Hore et al.[9] predict that the change in polymer conformation as a function of distance from the NP core is expected to be continuous, and

Received: March 23, 2018
Accepted: May 29, 2018
Published: May 31, 2018

DOI: 10.1021/acsmacrolett.8b00223
ACS Macro Lett. 2018, 7, 699−704

not change sharply at the CPB/SDPB interface. Thus, the two conformations observed in the CPB and SDPB regions[5−13] likely represent average conformations in the two concentration regimes.

Relatively little attention has been paid to the relaxation dynamics of polymer-grafted nanospheres. Work from the Archer group[16] utilized broadband dielectric spectroscopy (BDS) to probe the relaxation dynamics of the matrix polymer in polymer nanocomposites composed of polyisoprene (PI) or polybutadiene-grafted (PBD) SiO_2 NPs. The authors found NPs affect relaxation times in the host polymer, and act as plasticizers. Another study[17] probed the relaxation dynamics of PI-grafted SiO_2 NPs as a function of molecular weight via BDS, and found that grafting chains to spherical NPs can have a significant impact on the dynamics. Relaxation times for short chains were observed to be several orders of magnitude larger than those for untethered chains. As the molecular weight of the chains increased, the relaxation times for the grafted chains approached that of the untethered chains. The particles with the slowest relaxation times were observed to have large rubbery plateaus in the storage modulus as compared to those with shorter relaxation times, demonstrating the importance of grafted chain dynamics on the mechanical properties of polymeric materials. Jiang et al.[18] used NSE to understand the dynamics of polybutadiene chains that were bound to carbon black filler particles, and found evidence of "breathing modes" in the bound polymers. Another study[19] used a combination of SANS and NSE to study the dynamics of poly(ethylene oxide) adsorbed to clay platelets, finding evidence of a mobile and immobile regions of the adsorbed polymer chains. The mobile fraction of the chains exhibited Zimm dynamics, whereas the regions of the chains near the platelet surface were found to be immobile. Most recently, work from Krishnamoorti et al.[20] investigated the relaxation dynamics of polystyrene-grafted silica NPs in solutions of linear polystyrene using a combination of SANS and NSE. Because of the low grafting density, the brush would not have distinct CPB and SDPB regions. At short time scales, the dynamics of the grafted chains followed the Zimm model, but at longer time scales, the authors found that the chains deviated from Zimm behavior due to confinement effects. As free polymer was added into the system, the grafted polymers collapsed, resulting in increased confinement and slower dynamics. In this Letter, we report the measurement of the structure and relaxation dynamics of the CPB and SDPB regions of poly(methyl acrylate) (PMA) grafted SiO_2 NPs in solution, using SANS and NSE spectroscopy, by selectively deuterating each region of the brush. The measurements provide new insight into the local dynamics of the polymer brush as a function of distance from the NP core, and directly confirm the predicted structure of the grafted polymer layer.

Silica NPs were obtained from Nissan, Inc. (ORGANO-SILICASOL MIBK-ST) as a 30% solution by mass in methyl ethyl keytone and grafted with poly(methyl acrylate) (PMA) by surface-initiated RAFT. The polymer grafting was $\sigma = 0.3$ chains/nm^2. From eq 1, and the measured size of our SiO_2 NPs ($r_{core} \approx 4.5$ nm), we estimated that $h_{CPB} = r_c - r_{core} \approx 12$ nm. Using the Kuhn monomer[21] molar mass of $M_0 = 494.6$ g/mol and the Kuhn length $b = 1.5$ nm, the predicted molecular weight of the CPB region should be approximately 25 kg/mol. CPB dynamics were probed in sample PMA(h_6)-*b*-PMA(h_3d_3), which consisted of a 16.6 kg/mol hydrogenated PMA block (hPMA) ($Đ = 1.08$), followed by a 5.6 kg/mol deutereated PMA block (dPMA). SDPB dynamics were probed in sample PMA(h_3d_3)-*b*-PMA(h_6), which consisted of an 18.6 kg/mol dPMA block ($Đ = 1.07$), followed by a 20.3 kg/mol hPMA block. For both samples, the dispersity of the entire polymer was $Đ < 1.3$. The molecular weight of the hydrogenated block was chosen to be higher in sample PMA(h_3d_3)-*b*-PMA(h_6) to increase the scattering intensity, however this is not expected to affect the measurement results since relaxation times determined from NSE are length scale dependent, and values obtained at similar values of q correspond to similar length scales. Polymer-grafted NPs were dissolved in 1,1,2,2-tetrachloroethane-d_2 at a mass fraction of 4% for neutron scattering measurements. (***Warning!*** 1,1,2,2-tetrachloroethane is highly toxic and a possible carginogen) The full experimental methods are contained in the Supporting Information.

To directly probe the average conformation of the grafted PMA chains in the CPB and SDPB regions, the SANS data were fit to a core-chain-chain (CCC) model, which describes scattering from a spherical core grafted with polymers that have two regions, each with a different size, conformation, and scattering length density (SLD). The motivation for developing such a model comes from the observation of two regions of conformation,[5−7,9] as well as the presence of two regions with varying scattering length density in the brush. Under the CCC model, scattering from the spherical core is given by

$$P_{core}(q) = \left|F_{core}(q)\right|^2 = \left|V_{core}(\rho_c - \rho_s)\frac{3j_1(qr_{core})}{qr_{core}}\right|^2 \quad (2)$$

where $j_1(qr_{core})$ is a spherical Bessel function, r_{core} is the core radius, ρ_c and ρ_s are the SLDs of the core and solvent, respectively, and V_{core} is the volume of the core. Scattering from the polymer chains in the CPB and SDPB are separately described by their respective form factors, $P_{CPB}(q)$ and $P_{SDPB}(q)$, and their form factor amplitudes $F_{CPB}(q)$ and $F_{SDPB}(q)$. The form factor amplitude for a polymer chain in region i, with excluded volume and a radius of gyration $R_{g,i}$, is given by

$$F_i(q) = V_i(\rho_i - \rho_s)\frac{1}{2\nu_i U^{1/2\nu_i}}\gamma\left(\frac{1}{2\nu_i}, U\right) \quad (3)$$

where γ is the lower incomplete gamma function, V_i is the volume of the chain in region i, ν_i is the excluded volume parameter of the chain in region i, ρ_i is the SLD of the polymer in region i, and $U = q^2R_{g,i}{}^2(2\nu_i + 1)(2\nu_i + 2)/6$. The form factor of a polymer chain in region i is similar to the form factor amplitude:

$$P_i(q) = V_i^2(\rho_i - \rho_s)^2\left[\frac{1}{\nu_i U^{1/2\nu_i}}\gamma\left(\frac{1}{2\nu_i}, U\right) - \frac{1}{\nu_i U^{1/\nu_i}}\gamma\left(\frac{1}{\nu_i}, U\right)\right] \quad (4)$$

The total scattered neutron intensity is a combination of the form factors of the respective regions of the particle, and cross terms that describe correlations between distinct regions:

DOI: 10.1021/acsmacrolett.8b00223
ACS Macro Lett. 2018, 7, 699−704

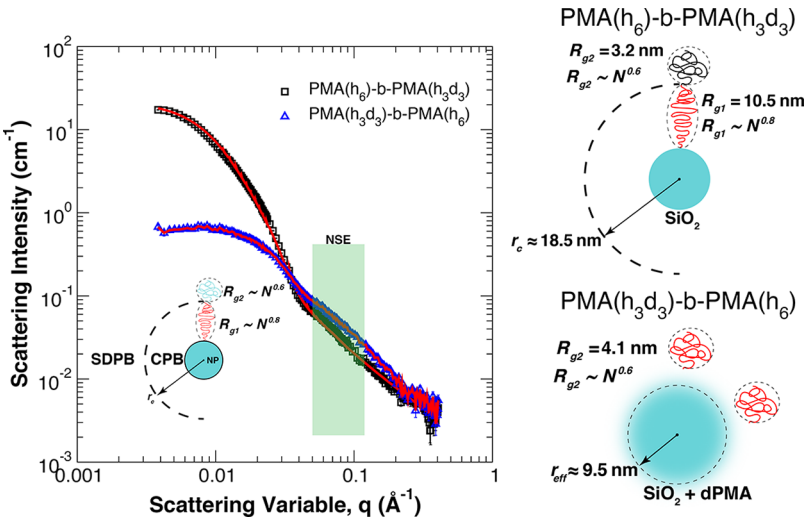

Figure 1. SANS from samples PMA(h_6)-*b*-PMA(h_3d_3) and PMA(h_3d_3)-*b*-PMA(h_6), along with fits to the core-chain-chain (CCC) model and a modified core-chain model. The inset shows the structure of the grafted PMA brush, and the two illustrations on the right depict the structures seen by neutron scattering due to contrast matching with the 1,1,2,2-tetrachloroethane-d_2 solvent, as interpreted from the fits to the SANS intensity. The shaded box is the region probed by NSE measurements. Error bars correspond to one standard deviation.

$$I(q) = \phi[P_{core}(q) + N_c P_{CPB}(q) + N_c P_{SDPB}(q) + 2N_c F_{core}(q) j_0(qr_{core}) F_{CPB}(q) + 2N_c F_{core}(q) j_0(qr_c) F_{SDPB}(q) + N_c(N_c - 1) F_{CPB}(q)^2 j_0(qr_{core})^2 + N_c(N_c - 1) F_{SDPB}(q)^2 j_0(qr_c)^2 + N_c^2 F_{CPB}(q) j_0(qr_{core}) j_0(qr_c) F_{SDPB}(q)] + B \quad (5)$$

where B is the incoherent background, r_c is the cutoff distance between the CPB and SDPB regions, j_0 is a propagator function represented by spherical Bessel function, and ϕ is the NP volume fraction.

SANS measurements of PMA-grafted SiO_2 NPs are shown in Figure 1, along with fits (red lines) to the CCC model eq 5. The inset of the graph depicts the assumed structure of the brush. Because the nanoparticles were dissolved in 1,1,2,2-tetrachloroethane-d_2, which has a SLD ($\rho_s \approx 3.708 \times 10^{-6}$ Å^{-2}) that is very close to that of SiO_2 ($\rho_{SiO_2} \approx 3.3 \times 10^{-6}$ Å^{-2}) and PMA(h_3d_3) ($\rho_{h_3d_3} \approx 3.875 \times 10^{-6}$ Å^{-2}), the SANS measurements are sensitive primarily to the regions of the chains that are fully hydrogenated ($\rho_{h_6} \approx 1.345 \times 10^{-6}$ Å^{-2}), with minimal scattering from the SiO_2 core and partially deuterated polymer. Sample PMA(h_6)-*b*-PMA(h_3d_3) (black squares) is deuterated such that scattering is from the CPB region. Fits to the SANS intensity reveal a cutoff distance $r_c = 18.5 \pm 0.3$ nm, implying a CPB region of approximately $h_{CPB} \approx 12$ nm. The chains in the CPB region are highly stretched, with $R_{g1} = 10.5 \pm 0.3$ nm and an excluded volume parameter very close to $\nu = 0.8$, in agreement with scaling theories. The fit was not very sensitive to the R_g of the polymer in the SDPB region due to low contrast. Using the Kuhn monomer molar mass and the Kuhn length,[21] we estimated that $R_{g2} = 2.5$ nm using $\nu = 0.6$. The best fit yielded $R_{g2} = 3.2 \pm 0.3$ nm. The schematic on the top right of Figure 1 illustrates the structure of the particles as determined by fitting the SANS data.

In contrast, sample PMA(h_3d_3)-*b*-PMA(h_6) is deuterated such that scattering comes primarily from the portion of the polymer in the SDPB region (blue triangles). Because of low contrast between the core, CPB, and solvent, fits of the SANS intensity to the CCC model were not satisfactory. The red curve is the fit to an approximation that treats the system as mixture of two components: spheres representing the effective nanoparticle + CPB core (eq 2) and polymer chains with excluded volume (eq 4). Because of poor contrast, the SANS spectra are not very sensitive to the former component and, therefore, the value obtained for its size should be considered only as an estimate. The scale of each component in the final scattering model was set according to the relative amounts of nanoparticles to grafted polymer chains, and resulted in a satisfactory fit to the data. The structure determined by SANS in shown in the schematic in the lower right of Figure 1. The radius of gyration of the chain in the SDPB region was $R_{g2} = 4.1 \pm 0.3$ nm with an excluded volume parameter $\nu = 0.6$, which is in excellent agreement with the value expected on the basis of the Kuhn molar mass and Kuhn length. Thus, the SANS measurements confirm both the structure of our particles as well as the sensitivity of NSE to the dynamics of the polymer chains in the CPB and SDPB regions of the brush.

The dynamics of the CPB and SDPB regions were probed separately by NSE spectroscopy of the same samples. The window of values of q that were probed by NSE is highlighted in the green box in Figure 1. NSE measurements were taken at $T = 80$ °C for $q = 0.058$ Å^{-1} to $q = 0.165$ Å^{-1}, and for Fourier times up to 40 ns. A subset of these measurements is shown in Figure 2, where the open points and dashed lines represent the measurement and fitting of dynamics in the CPB region, respectively. Closed points and solid lines correspond to measurements of the SDPB region. The normalized intermediate scattering function $I(q,t)/I(q,0)$ was fit to the Kohlrausch–Williams–Watts (KWW) function, with an added term to account for nanoparticle diffusion in solution:

$$\frac{I(q,t)}{I(q,0)} = A \exp\left[-\left(\frac{t}{\tau_q}\right)^{\beta}\right] \exp(-Dq^2 t) \quad (6)$$

where τ_q is the characteristic relaxation time at the scattering vector q, D is the nanoparticle diffusion coefficient, and A is a constant near unity. D and R_h were determined at $T = 25$ °C for both systems by dynamic light scattering (DLS), and found to

DOI: 10.1021/acsmacrolett.8b00223
ACS Macro Lett. 2018, 7, 699–704

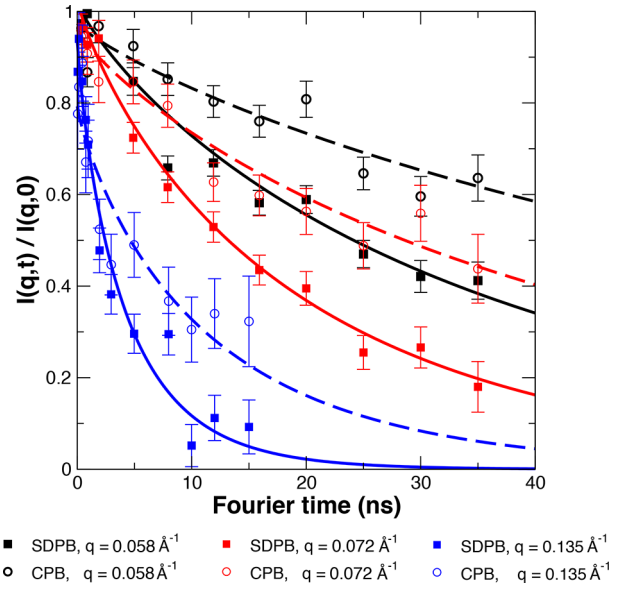

Figure 2. NSE measurements from PMA(h_6)-*b*-PMA(h_3d_3) and PMA(h_3d_3)-*b*-PMA(h_6). Solid points represent measurements of the dynamics of the SDPB region and open points represent measurements of the dynamics of the CPB region. Lines are fits to eq 6. Error bars correspond to one standard deviation.

be $D = (3.4 \pm 0.4) \times 10^{-8}$ cm^2/s for sample PMA(h_6)-*b*-PMA(h_3d_3) ($R_h = 43 \pm 5$ nm), and $D = (3.2 \pm 0.8) \times 10^{-8}$ cm^2/s for sample PMA(h_3d_3)-*b*-PMA(h_6) ($R_h \approx 46 \pm 11$ nm). Data were scaled to $T = 80$ °C using the Stokes–Einstein relation and the temperature-dependent viscosity for 1,1,2,2-tetrachloroethane. Depending on the value of β, eq 6 can capture either Rouse-like ($\beta = 0.5$) or Zimm-like ($\beta = 0.85$) dynamics.[22] Fitting yielded values of $\beta \approx 0.85$, implying Zimm-like dynamics rather than Rouse-like dynamics. Breathing modes are characterized by a fast decay of $I(q,t)/I(q,0)$, followed by a long plateau.[23] We do not see this feature, and can recover the solvent viscosity from the relaxation times in the SDPB region as $\eta_s = k_BT\tau_q q^3/6\pi \approx 0.0015$ Pa s, implying that the Zimm model is accurately describing the dynamics in the system.[24] Qualitatively, Figure 2 shows that the decay of the intermediate scattering function is slower in the CPB region than in the SDPB region, highlighting different dynamics in each region of the polymer brush.

The relaxation times determined from the intermediate scattering function are plotted in Figure 3 as a function of scattering variable q. At the smallest value of $q = 0.058$ Å^{-1}, which is sensitive to dynamics at the largest accessible length scales, the relaxation times of the CPB and SDPB differ by a factor of 2.5, with $\tau_q = 94.7 \pm 10.9$ ns for the CPB and $\tau_q = 35.7 \pm 2.0$ ns for the SDPB. As q increases, the relaxation times decrease as smaller length scales are measured. For both the CPB and SDPB, the relaxation times decrease and then begin to plateau near $q \approx 0.12$ Å^{-1}. τ_q for the CPB region remains approximately an order of magnitude greater than that of the SDPB region ($\tau_q \approx 15$ ns versus $\tau_q \approx 5$ ns). At the highest value of $q = 0.165$ Å^{-1}, NSE is sensitive to the dynamics on length scales of approximately 4 nm—corresponding to only a couple of Kuhn segments. Although it is reasonable that the relaxation times of the CPB and SDPB regions differ at large length scales, the observation of longer τ_q in the CPB region, at higher values of q, implies that even at very short length scales in the brush, the presence of neighboring chains significantly slows the dynamics in the CPB. The slowing of dynamics may be due to the spatial confinement of the chains as well as entanglements, since the molecular weight of the CPB region is above the entanglement molecular weight of PMA ($M_e = 11$ kg/mol).[21] An estimate of the monomer concentration c in the CPB region, relative to the overlap concentration c^*, finds $c/c^* \approx 10$, implying entanglements may play a role in slowing the dynamics. This observation can be substantiated by considering the scaling of the relaxation times with q. The inset of Figure 3 plots the relaxation times on a double logarithmic scale. If the dynamics in the polymer layer follow the Zimm model, $\tau_q \sim q^{-3}$. The data scale as $q^{-2.5}$ at low q (large length scales), however in the CPB region, a small deviation from Zimm-like behavior is observed at high q where the values plateau. The SDPB region follows Zimm-like behavior at all length scales measured in this study. The presence of Zimm-like dynamics in

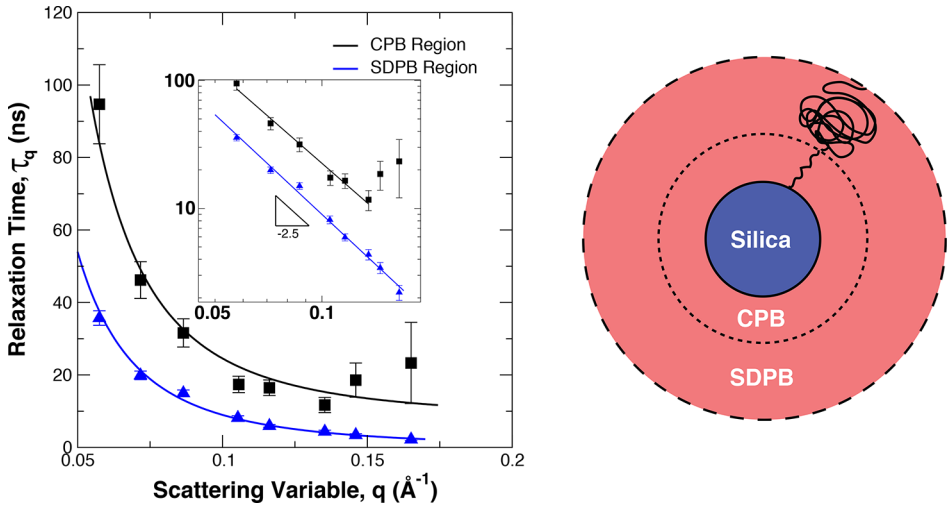

Figure 3. Characteristic relaxation times τ_q for the CPB region (squares) and SDPB region (triangles), as a function of scattering variable q. Solid lines are guides to the eye. The inset shows the same data on a double logarithmic plot. The slope of the blue line (SDPB region) is −2.5, indicating Zimm-like dynamics. Dynamics in the CPB region deviate from Zimm-like behavior at high q (small length scales). Error bars correspond to one standard deviation. The schematic on the right illustrates the CPB and SDPB regions being probed.

DOI: 10.1021/acsmacrolett.8b00223
ACS Macro Lett. 2018, 7, 699–704

both the CPB and SDPB regions can be rationalized in the context of work by Schneider et al.[25] of PEG adsorbed on SiO_2 nanoparticles. For this case, the authors surmised that elementary relaxation rates may not change due to confinement, but select modes, such as diffusion, can be suppressed.

In summary, we have taken advantage of contrast match conditions to selectively probe structure and relaxation dynamics of the CPB and SDPB regions of the brush formed by grafting PMA from SiO_2 nanoparticles, using a combination of SANS and NSE. A new core-chain-chain (CCC) model is able to determine the size and conformation of the portions of the polymer in each region, and finds excellent agreement with an extended Daoud-Cotton model, as well as scaling relationships measured experimentally by DLS and TEM. The relaxation dynamics of the CPB region were found to be significantly slower than the SDPB region due to the increased confinement of the chains in the CPB region. Interestingly, this observation persisted as q increased, indicating that the confinement effects in the CPB were present at the smallest length scales we probed, equivalent to a few Kuhn segments. Looking to the future, these measurements hint at the ability to further tailor the behavior of polymeric materials by controlling the structure of grafted polymers, which in turn impacts local confinement, relaxation dynamics, and mechanical properties.

■ ASSOCIATED CONTENT

Supporting Information

The Supporting Information is available free of charge on the ACS Publications website at DOI: 10.1021/acsmacrolett.8b00223.

Experimental methods, sample characterization, and python source code for the CCC model for implementation in SasView. (PDF)

■ AUTHOR INFORMATION

Corresponding Author

*(M.J.A.H.) E-mail: hore@case.edu.

ORCID

Michael J. A. Hore: 0000-0003-2571-2111

Notes

The authors declare no competing financial interest.

■ ACKNOWLEDGMENTS

Access to the NGA neutron spin echo spectrometer (NSE) and the NGB 30 m small-angle neutron scattering (SANS) instrument was provided by the Center for High Resolution Neutron Scattering (CHRNS), a partnership between the National Institute of Standards and Technology and the National Science Foundation under Agreement No. DMR-1508249. The identification of commercial products or experimental methods does not imply endorsement by NIST, nor does it imply that these are the best for the purpose. Y.W. and M.J.A.H. acknowledge partial support of this research by a National Science Foundation CAREER Award from the Polymers Program (DMR-1651002).

■ REFERENCES

(1) Kumar, S. K.; Jouault, N.; Benicewicz, B.; Neely, T. Nanocomposites with Polymer Grafted Nanoparticles. *Macromolecules* **2013**, *46*, 3199−3214.

(2) Hore, M. J. A.; Composto, R. J. Functional Polymer Nanocomposites Enhanced by Nanorods. *Macromolecules* **2014**, *47*, 875−887.

(3) Lee, P. W.; Isarov, S. A.; Wallat, J. D.; Molugu, S. K.; Shukla, S.; Sun, J. E. P.; Zhang, J.; Zheng, Y.; Lucius Dougherty, M.; Konkolewicz, D.; Stewart, P. L.; Steinmetz, N. F.; Hore, M. J. A.; Pokorski, J. K. Polymer Structure and Conformation Alter the Antigenicity of Virus-like Particle-Polymer Conjugates. *J. Am. Chem. Soc.* **2017**, *139*, 3312−3315.

(4) Lenart, W. R.; Hore, M. J. A. Structure-Property Relationships of Polymer-Grafted Nanospheres for Designing Advanced Nanocomposites. *Nano-Structures & Nano-Objects* **2017**, DOI: 10.1016/j.nanoso.2017.11.005.

(5) Ohno, K.; Morinaga, T.; Takeno, S.; Tsujii, Y.; Fukuda, T. Suspensions of Silica Particles Grafted with Concentrated Polymer Brush: Effects of Graft Chain Length on Brush Layer Thickness and Colloidal Crystallization. *Macromolecules* **2007**, *40*, 9143−9150.

(6) Dukes, D.; Li, Y.; Lewis, S.; Benicewicz, B.; Schadler, L.; Kumar, S. K. Conformational Transitions of Spherical Polymer Brushes: Synthesis, Characterization, and Theory. *Macromolecules* **2010**, *43*, 1564−1570.

(7) Choi, J.; Hui, C. M.; Schmitt, M.; Pietrasik, J.; Margel, S.; Matyjazsewski, K.; Bockstaller, M. R. Effect of Polymer-Graft Modification on the Order Formation in Particle Assembly Structures. *Langmuir* **2013**, *29*, 6452−6459.

(8) Choi, J.; Dong, H.; Matyjaszewski, K.; Bockstaller, M. R. Flexible Particle Array Structures by Controlling Polymer Graft Architecture. *J. Am. Chem. Soc.* **2010**, *132*, 12537−12539.

(9) Hore, M. J. A.; Ford, J.; Ohno, K.; Composto, R. J.; Hammouda, B. Direct Measurements of Polymer Brush Conformation Using Small-Angle Neutron Scattering (SANS) from Highly Grafted Iron Oxide Nanoparticles in Homopolymer Melts. *Macromolecules* **2013**, *46*, 9341−9348.

(10) Chevigny, C.; Gigmes, D.; Bertin, D.; Jestin, J.; Boué, F. Polystyrene Grafting from Silica Nanoparticles via Nitroxide-Mediated Polymerization (NMP): Synthesis and SANS Analysis with the Contrast Variation Method. *Soft Matter* **2009**, *5*, 3741−3753.

(11) Chevigny, C.; Jestin, J.; Gigmes, D.; Schweins, R.; Di-Cola, E.; Dalmas, F.; Bertin, D.; Boué, F. Wet-to-Dry" Conformational Transition of Polymer Layers Grafted to Nanoparticles in Nanocomposite. *Macromolecules* **2010**, *43*, 4833−4837.

(12) Chevigny, C.; Dalmas, F.; Di Cola, E.; Gigmes, D.; Bertin, D.; Boué, F.; Jestin, J. Polymer-Grafted-Nanoparticles Nanocomposites: Dispersion, Grafted Chain Conformation, and Rheological Behavior. *Macromolecules* **2011**, *44*, 122−133.

(13) Jouault, N.; Crawford, M. K.; Chi, C.; Smalley, R. J.; Wood, B.; Jestin, J.; Melnichenko, Y. B.; He, L.; Guise, W. E.; Kumar, S. K. Polymer Chain Behavior in Polymer Nanocomposites with Attractive Interactions. *ACS Macro Lett.* **2016**, *5*, 523−527.

(14) Robbes, A.-S.; Cousin, F.; Meneau, F.; Dalmas, F.; Schweins, R.; Gigmes, D.; Jestin, J. Polymer-grafted Magnetic Nanoparticles in Nanocomposites: Curvature Effects, Conformation of Grafted Chain, and Bimodal Nanotriggering of Filler Organization by Combination of Chain Grafting and Magnetic Field. *Macromolecules* **2012**, *45*, 9220−9231.

(15) Daoud, M.; Cotton, J. P. Star Shaped Polymers: A Model for the Conformation and Its Concentration Dependence. *J. Phys. (Paris)* **1982**, *43*, 531−538.

(16) Kim, D.; Srivastava, S.; Narayanan, S.; Archer, L. A. Polymer Nanocomposites: Polymer and Particle Dynamics. *Soft Matter* **2012**, *8*, 10813−10818.

(17) Kim, S. A.; Mangal, R.; Archer, L. A. Relaxation Dynamics of Nanoparticle-Tethered Polymer Chains. *Macromolecules* **2015**, *48*, 6280−6293.

(18) Jiang, N.; Endoh, M. K.; Koga, T.; Masui, T.; Kishimoto, H.; Nagao, M.; Satija, S. K.; Taniguchi, T. Nanostructures and Dynamics of Macromolecules Bound to Attractive Filler Surfaces. *ACS Macro Lett.* **2015**, *4*, 838−842.

DOI: 10.1021/acsmacrolett.8b00223
ACS Macro Lett. 2018, 7, 699−704

(19) Frielinghaus, X.; Brodeck, M.; Holderer, O.; Frielinghaus, H. Confined Polymer Dynamics on Clay Platelets. *Langmuir* **2010**, *26*, 17444−17448.
(20) Poling-Skutvik, R.; Olafson, K. N.; Narayanan, S.; Stingaciu, L.; Faraone, A.; Conrad, J. C.; Krishnamoorti, R. Confined Dynamics of Grafted Polymer Chains in Sollutions of Linear Polymer. *Macromolecules* **2017**, *50*, 7372−7379.
(21) Fetters, L. J.; Lohse, D. J.; Colby, R. H. Chain Dimensions and Entanglement Spacings. In *Physical Properties of Polymers Handbook*; Mark, J. E., Ed.; SpringerMaterials: 2007; pp 447−454.
(22) Richter, D.; Monkenbusch, M.; Arbe, A.; Colmenero, J. *Neutron Spin Echo in Polymer Systems*; Springer: Berlin, 2005.
(23) Farago, B.; Monkenbusch, M.; Richter, D.; Huang, J. S.; Fetters, L. J.; Gast, A. P. Collective Dynamics of Tethered Chains: Breathing Modes. *Phys. Rev. Lett.* **1993**, *71*, 1015.
(24) Kanaya, T.; Monkenbusch, M.; Watanabe, H.; Nagao, M.; Richter, D. Dynamics of Deuterated Polystyrene-Protonated Butadiene Diblock Copolymer Micelles by Neutron Spin Echo. *J. Chem. Phys.* **2005**, *122*, 144905.
(25) Glomann, T.; Schneider, G. J.; Allgaier, J.; Radulescu, A.; Lohstroh, W.; Farago, B.; Richter, D. Microscopic Dynamics of Polyethylene Glycol Chains Interacting with Silica Nanoparticles. *Phys. Rev. Lett.* **2013**, *110*, 178001.

DOI: 10.1021/acsmacrolett.8b00223
ACS Macro Lett. 2018, 7, 699−704